CrystEngComm

Accepted Manuscript

ROYAL SOCIETY OF CHEMISTRY

www.rsc.org/crystengcomm

Journal Name

COMMUNICATION

Temperature-Triggered Dielectric Switchable Material in a Perovskite-Type Cage Compound†

Received 20th June 2016,
Accepted 15th August 2016

DOI: 10.1039/x0xx00000x

www.rsc.org/

Kun Qian*,[a] Feng Shao,[b] Zhihong Yan,[b] Jie Pang,[c] Xiaodong Chen,[a] and Changxin Yang[a]

The perovskite-type cage compound $[C_3H_6NH_2]_2[KCo^{III}(CN)_6]$ shows a temperature-triggered dielectric switch. The switchable property around 199 K was revealed by crystal structure studies between low and high dielectric states. It derives from an order–disorder phase transition of the system, changing the motions of the polar azetidine cations guests.

Switchable materials, whose physical properties (optical, electrical or magnetic properties) can be reversibly modified between two or more relatively stable states by external stimuli such as light, temperature, and electric field, have attracted great attention for their wide application in the fields of photonic devices, optoelectronic technology, digital processing, sensors, etc[1–5]. Among various types of switchable materials, cage compounds which mimic the inorganic ABO_3-type perovskite-like structure, with inclusion of guest cations within the well-matched cage-like host frameworks, can undergo reversible structural phase transitions upon thermal stimulus, which can often lead to a change or a switch of the related physical properties[6–25]. An example is that cage compounds can undergo a transition between high and low dielectric states at a phase transition temperature (T_c). Basically, the switching of the dielectric constant at T_c is due to motional changes of polar molecules or ions between "rotating or hopping" (melt-like) and orientationally ordered (frozen) states, which correspond to a high-temperature phase (HTP) and low-temperature phase (LTP), respectively. However, reports of such cage compounds have remained scarce owing to a lack of knowledge regarding control of the motions of the dipole moments in the crystal lattice.

There still exist two significant challenges: one is how to control the switching response characteristics by structural modulation and external stimuli and the other is how to obtain compounds with switchable physical properties. One of the most feasible strategies is to construct temperature-triggered solid-to-solid structural phase transition materials, due to the fact that the physical properties often present abrupt changes near the phase transition temperature.[26–39] Cage compounds are a very promising class of switchable molecular dielectrics, in which dipolar reorientation can contribute significantly to the dielectric response, motions of the dipoles can be switched on or off by temperature. On the one hand, cage compounds have been proven to be excellent candidates to prepare phase transition materials.[40-52] On the other hand, the reorientations of the polar guests in the carefully designed cage compounds may give rise to large dielectric permittivity, which are characterized by a high-dielectric state, and their freezing will lead to low-dielectric systems.[13,53] Herein we present a novel organic–inorganic hybrid cage compound $[C_3H_6NH_2]_2[KCo^{III}(CN)_6]$ (**1**) with a perovskite-type structure, in which the order–disorder behavior of the polar azetidine (AZT) guests give rise to striking dielectric anomalies.

Compound **1** was synthesized as colorless block-shaped crystals by slowly layering a methanol solution of $[C_3H_6NH_2]Cl$ salts into an aqueous solution of $K_3[Co(CN)_6]$ and Na_2CO_3 in the ratio of 1:1:4 (see the Supporting Information). The existence of AZT and CN groups in **1** is verified by IR spectra (Figure S1). Strong IR bands centered at 2116 cm^{-1} can be assigned to ν(C–N) stretching vibration of CN^- ligand. Medium IR bands centered at 3203 cm^{-1} can be assigned to the ν(N–H) stretching modes of NH_2^+ group. The NH_2^+ deformation vibrations were observed at 1594.8 and 1453.6 cm^{-1}.

The phase transition behavior of **1** was first evidenced by the DSC measurements. The curve of DSC was tested at the temperature ranging from 160 to 230 K with a heating/cooling rate of 10 K/min under nitrogen atmosphere (Figure 1). One anomaly is detected at 199 / 196 K (T_c) during the heating/cooling processes, indicating that **1** undergoes a reversible phase transition with a small thermal hysteresis of 3 K. The small thermal hysteresis and the sharp anomalous peaks support the discontinuous character of the transition, indicative of a first-order phase transition. For

[a] College of Pharmacy, Jiangxi University of Traditional Chinese Medicine, Nanchang, 330004 P. R. China. E-mail: qk0876@hotmail.com
[b] Key Laboratory of Modern Preparation of TCM, Ministry of Education, Jiangxi University of Traditional Chinese Medicine, Nanchang 330004, P. R. China
[c] State Key Laboratory of Analytical Chemistry for Life Science, School of Chemistry and Chemical Engineering, Nanjing University, Nanjing, 210023 P. R. China

† Electronic Supplementary Information (ESI) available: Materials and instrumentations, synthesis, Single crystal X-ray crystallography, IR spectrum, TGA spectrum, Dielectric spectrum, crystallographic data, and selected bond and angle. CCDC 998555 at 173 K and 998556 at 298 K. For crystallographic data in CIF or other electronic format See DOI: 10.1039/x0xx00000x

convenience, we label the phase above T_c as the high-temperature phase (HTP), and the phase below T_c as low-temperature phase (LTP).

To understand the structural phase transition, a variable-temperature single-crystal X-ray diffraction (XRD) study of **1** was performed in the range 113-293 K. It reveals that **1** crystallizes in the cubic space group $Fm\bar{3}m$ at 113 K and $Pm\bar{3}m$ at 293 K, respectively (Table S1). The most striking structural feature is the double perovskite structure, known as cyano-elpasolites $A_2[B' B''(CN)_6]$ (A=monovalent cation, B' (I) =monovalent metal, and B'' (III) = trivalent metal), in which the cationic A guest is located in the cage formed by B' –NC–B'' (Figure 2). The structural difference between the HTP and LTP can mainly be attributed to the different motion modes of the AZT guest as well as a small change in volume of the $[K_4Co_4(CN)_{12}]$ cage, which leads to the structural phase transition.

The structure at 293 K (HTP) belongs to the cubic space group $Pm\bar{3}m$, with a= b= c = 11.823(1) Å. In **1**, the anionic cage is formed by Co–CN–K units (Figure 2 on the left). There are two different kinds of Co^{2+} ions and K^+ ions in the crystal lattice. The metal–cyanide bond is strong and covalent in the fragment $Co(CN)_6$ (The distances of Co–C bonds are range from 1.884 to 1.930 Å) and much weaker and ionic in the fragment $K(NC)_6$ (The distances of K–N bonds are from 2.827 to 2.898 Å) (Table S2). One K^+ ion adopts an octahedral coordination geometry compressed along the *c* axis, with equatorial K–N = 2.832 Å and apical K–N = 2.827 Å. The other K^+ ions adopt an octahedral coordination geometry along the *c* axis, with each K–N = 2.898 Å. Each $[K_4Co_4(CN)_{12}]$ cage accommodates a AZT cation that displays orientational disorder over six sites. The AZT cation consists of three carbon atoms and one nitrogen atom, of which two carbon atoms shows disorder only over six sites. The AZT cation reorients around the sixfold axis perpendicular to the ring plane. The site occupancies of the two disorder C atoms are 0.167 respectively. It should be noted that the AZT cation in the HTP was disordered shown as tetrahexahdron, revealing the existence of a highly dynamically disordered cation.

However, the crystal structure at 113 K (LTP) adopts the cubic space group $Fm\bar{3}m$ with similar cell parameters of a = b = c = 11.759(7) Å. In **1**, the anionic cage is formed by Co–CN–K units as well as in the HTP (Figure 2 on the right). The characteristics of metal–cyanide bond in the fragment of $Co(CN)_6$ and $K(NC)_6$ were found to be the same as the above-mentioned in the HTP, except that the distance of Co–C (Co–C ≈ 1.881 Å) and K–N (K–N ≈ 2.863 Å) changed slightly (Table S3). Each K^+ ion adopts an octahedral coordination geometry along the *c* axis, with K–N = 2.863 Å. Each $[K_4Co_4(CN)_{12}]$ cage accommodates a AZT cation that displays orientational disorder over two sites. The AZT cation consists of one nitrogen atom and three carbon atoms, of which two carbon atoms were all refined as carbon-nitrogen atoms. For each atom of the guest cation, a disorder was shown at only two sites with equal occupancy (Figure 2 on the right). The site occupancies of the two C atoms are 0.50. The site occupancies of the other two atoms are 0.5, divided into 0.25 of C and 0.25 of N respectively. Contrarily, the AZP cation in the LTP is frozen out to be ordered over two sites at 113 K shown as a cube.

It is known that disorder–order transition is one of the origins of phase transitions. From the above structural analysis, it is clear that the most notable difference between the HTP and LTP is the disorder-order transition of AZT cations. The structure at 293 K (HTP) belongs to the cubic space group $Pm\bar{3}m$, with a= b= c = 11.823(1) Å. The crystal structure at 113 K (LTP) belongs to the space group $Fm\bar{3}m$ with a = b = c= 11.759(7) Å. As a result, the volume of the $[K_4Co_4(CN)_{12}]$ cage in the HTP is more than 1.7 % in the LTP. The AZT cations are orientationally disordered over two sites in the LTP, while six independent disordered AZT cations can be found in the HTP. It appears that the disorder–order transition of the AZT cations is responsible for the phase transition at 199 K. During the phase transiton, the symmetry of the system is broken. The AZT guest is shown as a cube in the LTP, while a tetrahexahdron in the HTP.

Differential scanning calorimetry (DSC) measurements in the temperature range 160–230 K (Figure 1) indicate a structural phase transition of **1** at 199 K. The sharp peaks and the thermal hysteresis in the DSC curves show the characteristics of a first-order phase transition. From the DSC curves, the value of ΔH_{mol} is 6.69 J mol $^{-1}$ at 199 K. The entropy increase, ΔS around T_c is 32.5 J K^{-1} mol^{-1}. An estimate of the number of molecular orientations from the calorimetric data yields N = 50, based on the Boltzmann equation, $\Delta S = R\ln(N)$, where R is the gas constant and *N* is the ratio of the numbers of respective geometrically distinguishable orientations in both phases. This indicates that the AZT cations are much more disordered in the HTP than in the LTP, consistent with the single-crystal XRD data discussed above.

Dielectric constant measurement was performed on the powdered samples **1** in the range 120-270 K and 1-1000 kHz (Figure 3; Supporting Information). There is no evidence of frequency dependence in the measured frequency range (Figure S2, Figure S3). Upon heating, the real part ε' keeps stable below 199 K with a value of about 6, which corresponds to a low-dielectric state. Then it sharply increases at 199 K, the ε' value increases to reach a peak value of about 17. Above 199 K, the ε' keeps stable with a value of 17, which corresponds to a high-dielectric state (Figure 3). This trend reflects the competition between orientational polarization upon electric field and random thermal motion of the AZT cations. A rapid increase is followed to a value of about 17 at 199 K, which corresponds to a transition from the low-dielectric state to the high-dielectric state. These dielectric changes are associated with the static-motional transitions of the polar AZT cations in the crystal. It undergoes a static disorder over two sites that does not contribute to the dielectric constant in the LTP. However, it shows a dynamic disorder over six sites that contributes to the dielectric constant in the HTP. The transition between high dielectric state and low dielectric state is ascribed to a partial activation of the polar AZT cation.

In summary, a perovskite-type cage compound $[C_3H_6NH_2]_2[KCo^{III}(CN)_6]$ was synthesized and characterized as temperature-triggered switchable dielectric materials. It exhibits one phase transitions around 199 K. An order–disorder mechanism is found in the structural transformations owing to the motions of the cationic guests under different temperatures. Investigations on such systems can help to understand structural phase transitions of switchable molecular dielectrics and afford a useful strategy in searching for new electric ordering materials.

This work was supported by the Doctoral Research Starting Foundation for Jiangxi university of Traditional Chinese Medicine (No. 2014BS005), National Natural Science Foundation of China (Grants 81260638).

Notes and references

[1] Feringa, B. L.; van Delden, R. A.; Koumura, N.; Geertsema, E. M. *Chem. Rev.* **2000**, *100*, 1789-1816.
[2] Champagne, B.; Plaquet, A.; Pozzo, J. L.; Rodriguez, V.; Castet, F. *J. Am. Chem. Soc.* **2012**, *134*, 8101-8103.
[3] Raymo, F. M. *Adv. Mater.* **2002**, *14*, 401-414.
[4] Irie, M.; Fukaminato, T.; Sasaki, T.; Tamai, N.; Kawai, T. *Nature*, **2002**, *470*, 759-760.
[5] Kawata, S.; Kawata, Y. *Chem. Rev.* **2000**, *100*, 1777-1788.
[6] Wang, Z.; Zhang, B.; Otsuka, T.; Inoue, K.; Kobayashi, H.; Kurmoo, M. *Dalton Trans*. **2004**, 2209-2216.
[7] Jain, P.; Dalal, N. S.; Toby, B. H.; Kroto, H. W.; Cheetham, A. K. *J. Am. Chem. Soc*. **2008**, *130*, 10450-10451.
[8] Kojima, A.; Teshima, K.; Shirai, Y.; Miyasaka, T. *J. Am. Chem. Soc.* **2009**, *131*, 6050– 6051.
[9] Zhang, W.; Cai, Y.; Xiong, R.-G.; Yoshikawa, H.; Awaga, K. *Angew. Chem. Int. Ed.* **2010**, *49*, 6608-6610; *Angew. Chem.* **2010**, *122*, 6758-6760.
[10] Fu, D.-W.; Zhang, W.; Cai, H.-L.; Zhang, Y.; Xiong, R.-G.; Huang, S. D.; Nakamura, T. *Angew. Chem. Int. Ed.* **2011**, *50*, 11947–11951; *Angew. Chem*. **2011**, *123*, 12153-12157.
[11] Takahashi, Y.; Obara, R.; Lin, Z.-Z.; Takahashi, Y.; Naito, T.; Inabe, T.; Ishibashi, S.; Terakura, K. *Dalton Trans*. **2011**, *40*, 5563-5568.
[12] Asaji, T.; Ito, Y.; Seliger, J.; Žagar, V.; Gradišek, A.; Apih, T. *J. Phys. Chem. A* **2012**, *116*, 12422– 12428.
[13] Zhang, W.; Ye, H.-Y.; Graf, R.; Spiess, H. W.; Yao, Y.-F.; Zhu, R.-Q.; Xiong, R.-G. *J. Am. Chem. Soc*. **2013**, *135*, 5230-5233.
[14] Li, W.; Thirumurugan, A.; Barton, P. T.; Lin, Z.; Henke, S; Yeung, H. H.-M.; Wharmby, M. T.; Bithell, E. G.; Howard, C. J.; Cheetham, A. K. *J.Am. Chem. Soc.* **2014**, *136*, 7801-7804.
[15] Maczka, M.; Pietraszko, A.; Macalik, B.; Hermanowicz, K. *Inorg. Chem.* **2014**, *53*, 787– 794.
[16] Maczka, M.; Ciupa, A.; Gagor, A.; Sieradzki, A.; Pikul, A.; Macalik, B.; Drozd, M. *Inorg. Chem.* **2014**, *53*, 5260– 5268.
[17] Kazim, S.; Nazeeruddin, M. K.; Nazeeruddin, M. K.; Grätzel, M.; Ahmad, S. *Angew. Chem. Int. Ed.* **2014**, *53*, 2812– 2824; *Angew. Chem.* **2014**, *126*, 2854– 2867.
[18] Du, Z.-Y.; Zhao, Y.-P.; Zhang, W.-X.; Zhou, H.-L.; He, C.-T.; Xue, W.; Wang, B.-Y.; Chen, X.-M. *Chem. Commun.* **2014**, *50*, 1989.
[19] Shi, C.; Zhang, X.; Cai, Y.; Yao, Y.-F.; Zhang, W. *Angew. Chem. Int. Ed.* **2015**, *54*, 1-6.
[20] Chen,T.-L.; Zhou, Y.-L.; Sun, Z.-H.; Zhang, S.-Q.; Zhao, S-G.; Tang, Y-Y.; Ji, C.-M. Luo, J.-H. *Inorg. Chem.* **2015**, *54*, 7136-7138.
[21] Du, Z.-Y.; Xu, T.-T.; Huang, B.; Su, Y.-J.; Xue, W.; He, C.-T.; Zhang, W.-X.; Chen, X.-M. *Angew. Chem. Int. Ed.* **2015**, *54*, 914-918; *Angew. Chem*. **2015**, *127*, 928-932.
[22] Liao, W.-Q.; Ye, H.-Y.; Zhang, Y.; Xiong, R.-G. *Dalton Trans.* **2015**, *44*, 10614-10620.
[23] Shi, C.; Yu, C.-H.; Zhang, W. *Angew. Chem. Int. Ed.* **2016**, *55*, 5798-5802; *Angew. Chem.* **2016**, *128*, 5892-5896
[24] Xu, W.-J.; Chen, S.-L.; Hu, Z.-T.; Lin, R.-B.; Su, Y.-J.; Zhang, W.-X.; Chen, X.-M. *Dalton Trans.* **2016**, *45*, 4224-4229.
[25] Bermúdez-García, J. M.; Sánchez-Andújar, M.; Yáñez-Vilar, S.; Castro-García, S.; Artiaga, R.; López-Beceiro, J.; Botana, L.; Alegría, A.; Señarís-Rodríguez, M. A. *J. Mater. Chem. C*, **2016**, *4*, 4889-4898.
[26] Wriedt, M.; Yakovenko, A. A.; Halder, G. J.; Prosvirin, A. V.; Dunbar, K. R.; Zhou, H. C. *J. Am. Chem. Soc.* **2013,** *135,* 4040-4050.
[27] Sun, Z. H.; Luo, J. H.; Zhang, S. Q.; Ji, C. M.; Zhou, L.; Li, S. H.; Deng, F.; Hong, M. C. *Adv. Mater.* **2013**, *25*, 4159-4163.
[28] Zhang, Y.; Liao, W. Q.; Ye, H. Y.; Fu, D. W.; Xiong, R.-G. *Cryst.Growth Des*. **2013**, *13*, 4025-4030.
[29] Bi, W.; Louvain, N.; Mercier, N.; Luc, J.; Rau, I.; Kajzar, F.; Sahraoui, B. *Adv. Mater.* **2008**, *20*, 1013-1017.
[30] Shi, X. J.; Luo, J. H.; Sun, Z. H.; Li, S. G.; Ji, C. M.; Li, L. N.; Han, L.; Zhang, S. Q.; Yuan, D. Q.; Hong, M. C. *Cryst. Growth Des.* **2013**, *13*, 2081-2086.
[31] Zhao, X. H.; Huang, X. C.; Zhang, S. L.; Shao, D.; Wei, H. Y.; Wang, X. Y. *J. Am. Chem. Soc*. **2013**, 135, 16006-16009.
[32] Beekman, C.; Siemons, W.; Ward, T. Z.; Chi, M.; Howe, J.; Biegalski, M. D.; Balke, P.; Mksymovych, N.; Farrar, A. K.; Romero, J.B.; Gao, P.; Pan, W. Q.; Tenne, D. A.; Christen, H. M. *Adv. Mater.* **2013**, *25*, 5561-5567.
[33] Li, S. G.; Luo, J. H.; Sun, Z. H.; Zhang, S. Q.; Li, L. N.; Shi, X. J.; Hong, M. C. *Cryst. Growth Des*. **2013**, *13*, 2675-2679.
[34] Shi, P.-P.; Sun, S.-W.; Liu, M.-L.; Kong, L.-H.; Ye, Q. *Inorg. Chem. Commun.* **2013**, *37*, 84-88
[35] Tang, Y. Y.; Ji, C. M.; Sun, Z. H.; Zhang, S. Q.; Chen, T. L.; Luo, J. H. *Chem. Asian J.* **2014**, *9*, 1771-1776.
[36] Liao, W.-Q.; Ye, H.-Y.; Fu, D.-W.; Li, P.-F.; Chen, L.-Z.; Zhang, Y. *Inorg. Chem.* **2014**, *53*, 11146-11151
[37] Shi, C.; Zhang, X; Cai, Y.; Yao, Y.-F.; Zhang, W. *Angew. Chem. Int. Ed.* **2015**, *54*, 6206-6210; *Angew. Chem.* **2015**, *127*, 6304-6308
[38] Shao, X.-D.; Zhang, X.; Shi, C.; Yao, Y.-F.; Zhang, W. *Adv. Sci.* **2015**, *2*, 2198-3844.
[39] Zeng, S.-Y.; Sun, Z.-H.; Ji, C.-M.; Zhang, S.-Q.; Song, C.; Luo, J.-H. *Cryst. Eng. Comm.* **2016**, *18*, 3606-3611
[40] Xu, G. C.; Ma, X. M.; Zhang, L.; Wang, Z. M.; Gao, S. *J. Am.Chem. Soc*. **2010**, *132*, 9588-9590.
[41] Xu, G. C.; Zhang, W.; Ma, X. M.; Chen, Y. H.; Zhang, L.; Cai, H. L.; Wang, Z. M.; Xiong, R.-G.; Gao, S. *J. Am. Chem. Soc.* **2011**, *133*,14948-14951.
[42] Shang, R.; Xu, G. C.; Wang, Z. M.; Gao, S. *Chem. Eur. J.* **2014**, *20*, 1146−1158.
[43] Stoumpos, C. C.; Malliakas, C. D.; Kanatzidis, M. G. *Inorg.Chem.* **2013**, *52*, 9019-9038.
[44] Shang, R.; Xu, G.-C.; Wang, Z.-M.; Gao, S. *Chem. Eur. J.* **2014**, *20*, 1146-1158.
[45] Mączka, M.; Gągor, A.; Macalik, B.; Pikul, A.; Ptak, M.; Hanuza, J. *Inorg. Chem.* **2014**, *53*, 457-467.
[46] Han, J.; Nishihara, S.; Inoue, K.; Kurmoo, M. *Inorg. Chem.* **2014**, *53*, 2068-2075.
[47] Zhang, Y.; Ye, H. Y.; Zhang, W.; Xiong, R.-G. *Inorg. Chem. Front.* **2014**, *1*, 118-123.
[48] Chen, S.; Shang, R.; Hu, K.-L.; Wang, Z.-M.; Gao, S. *Inorg. Chem. Front.* **2014**, *1*, 83-98.
[49] Du, Z.-Y.; Sun, Y.-Z.; Chen, S.-L.; Huang, B.; Su, Y.-J.; Xu, T.-T.; Zhang, W.-X.; Chen, X.-M. *Chem. Commun.* **2015**, *51*, 15641-15644
[50] Zhang, X.; Shao, X.-D.; Li, S.-C.; Cai, Y.; Yao, Y.-F.; Xiong, R.-G.; Zhang, W. *Chem. Commun.* **2015**, *51*, 4568-4571
[51] Shang, R.; Wang, Z.-M.; Gao, S. *Angew. Chem. Int. Ed.* **2015**, *54*, 2534-2537; *Angew. Chem.* **2015**, *127*, 2564-2567.
[52] Liu, Y.-L.; Wang, Y.-F.; Zhang, W. *Cryst. Eng. Comm.* **2016**, *18*, 1958-1963.
[53] Yu, S.-S.; Liu, S.-X.; Duan, H.-B. *Dalton Trans.* **2015**, *44*, 20822-20825.

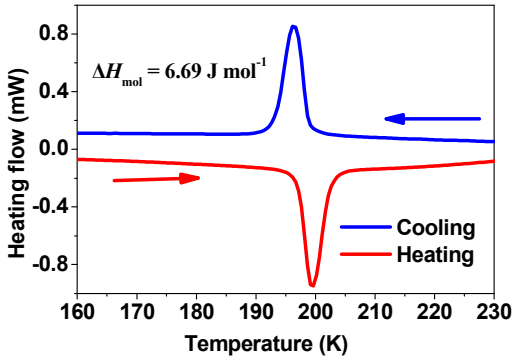

Figure **1**. DSC curves of **1** shown in the temperature range of 160-230 K.

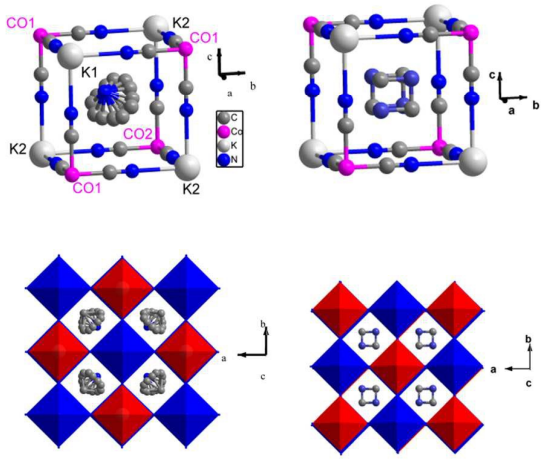

Figure **2**. Cage structures of **1** and packing diagrams viewed along the *c* axis and at 293 K on the left and 113 K on the right. All H atoms are omitted for clarity.

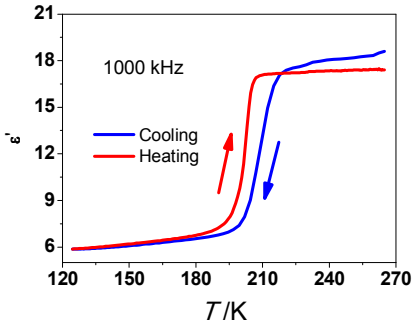

Figure 3. Dielectric constant curves of **1** at 1000 kHz.

Graphical abstract

A perovskite-type cage compound $[C_3H_6NH_2]_2[KCo^{III}(CN)_6]$ shows a temperature-triggered dielectric switch. The switchable property derives from an order–disorder phase transition of the system, changing the motions of the polar azetidine cations guests.